Analytic model for ring pattern formation by bacterial swarmers

Scott Arouh
Physics Department, University of California, San Diego, 9500 Gilman Drive, La Jolla, California 92093-0319
(Received 15 June 2000; published 27 February 2001)

We analyze a model proposed by Medvedev, Kaper, and Kopell (the MKK model) for ring formation in two-dimensional bacterial colonies of *Proteus mirabilis*. We correct the model to formally include a feature crucial of the ring generation mechanism: a bacterial density threshold to the nonlinear diffusivity of the MKK model. We numerically integrate the model equations, and observe the logarithmic profiles of the bacterial densities near the front. These lead us to define a consolidation front distinct from the colony radius. We find that this consolidation front propagates outward toward the colony radius with a nearly constant velocity. We then implement the corrected MKK equations in two dimensions and compare our results with biological experiment. Our numerical results indicate that the two-dimensional corrected MKK model yields smooth (rather than branched) rings, and that colliding colonies merge if grown in phase but not if grown out of phase. We also introduce a model, based on coupling the MKK model to a nutrient field, for simulating experimentally observed branched rings.

DOI: 10.1103/PhysRevE.63.031908 PACS number(s): 87.18.Hf, 87.18.Ed, 87.18.Bb, 87.18.−h

I. INTRODUCTION

Colonies of bacteria growing on a hard surface have been observed to produce patterns of concentric rings. These rings form after inoculation of a bacterial culture in the center of a Petri dish containing nutrient-enriched agar, and allowing the bacteria to grow. Certain species of bacteria, such as *Proteus mirabilis* [1,2], *Vibrio parahaemolyticus* [3], and *Bacillus subtilis* [4], have been observed to form these terraced ring patterns during their colonial development under certain conditions. The challenge of modeling the formation of these ring patterns has stood unsolved for over a century [2].

These ring patterns form by way of a cyclic lifestyle of differentiation and dedifferentiation for the bacteria. During one stage of this cycle, initially short, relatively nonmotile bacteria increase in numbers by reproduction without significantly increasing the surface area of the colony. During the other stage of the cycle, some subset of the short bacteria differentiate into relatively long swarmer cells. These swarmers quickly increase the span of the colony by migrating outward from the colony edge as they grow. Once this swarming phase is complete, the change in bacterial density between the previous and newly occupied areas of the colony delineate a macroscopically observable boundary within the colony in the shape of the ring.

A number of biological observations are associated with the phenomenon of bacterial ring formation. Primary among these is that the rings form in bursts of growth by the rapid spreading of differentiated bacteria called *swarmers*, as illustrated in colony radius time series plots such as our simulation results of Fig. 1(b). The bacteria of a species capable of swarming are initially in the form of *swimmers*, relatively short rods that swim with one or a few rotating arms called flagella. When the motion of their flagella is inhibited by the presence of a highly viscous fluid or a hard substrate, the swimmers express an additional set of genes that inhibits septation (separation of mother and daughter cells during cell division) and (at least in *Vibrio*) codes for a structurally distinct type of flagellum [3]. The result of this differentiation process is a longer (typically 30 times longer [3] in *Vibrio* but only 1.5–2 times longer [4] in the branched rings of *Bacillus*), hyperflagellated cell, a swarmer. This process is illustrated in Fig. 2. Swarmer cells interact with each other much more so than swimmer cells. The flagella of adjacent swarmers become entangled, which locks both cells in the same orientation. In this way, groups of swarmers become linked together into rafts of bacteria, all with the same orientation of their long axis: these rafts move as single units. Through an unidentified mechanism, these rafts of bacteria expand the colony radius much more quickly than the composite motions of noninteracting swimmer cells. A primary goal of modeling these ring patterns is to understand how these swarmers use bacteria-bacteria interactions to move much more quickly than the swimmers.

Recent progress in modeling these bacterial ring patterns has yielded a framework for further analysis. Esipov and Shapiro recently proposed a kinetic model [5] incorporating a number of biological observations of these systems and reproducing (in one dimension) the bursts of growth observed experimentally. Their model explicitly incorporates an age distribution as well as a spatial distribution of bacteria. Although a dramatic improvement to the state of *Proteus* ring modeling and a very interesting mechanism, the Esipov-Shapiro model was inelegant and difficult to analyze. One difficulty was that the form in which they incorporated experimental observations was not amenable to mathematical analysis. Most of these factors were incorporated into the functional form of a diffusivity. The resulting diffusivity consisted of three experimentally motivated factors, including the use of a threshold to an additional motility field. Furthermore, the increase in dimensionality of the system associated with the use of a bacterial age distribution hindered simulation in the desired two spatial dimensions of the plate on which the bacteria grow.

Both of these problems were solved by Medvedev, Kaper, and Kopell's reformulation [6] of the Esipov-Shapiro model. They simplified the model to a system of two partial differential equations. They did this by averaging over the age

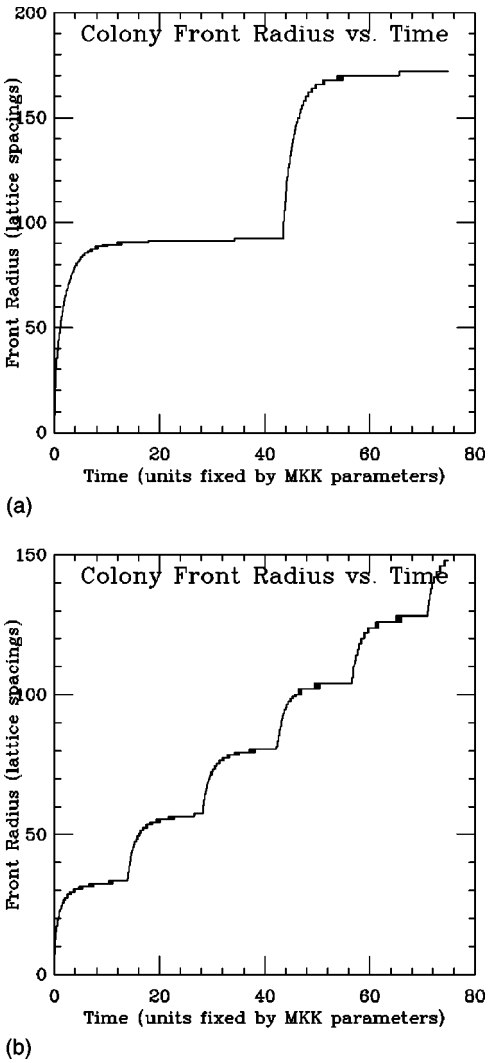

FIG. 1. Illustration of the effect on colony radius time series of varying the swarmer density diffusivity threshold. The swarmer density diffusivity threshold u_{thresh} of the diffusivity expression (2) is varied, and the colony radius time series plotted. (a) A large-period swarm plus consolidation cycle, due to a relatively small $u_{\text{thresh}}=10^{-10}$ in Eq. (2). We use this value of u_{thresh} elsewhere except where noted. (b) A smaller-period swarm plus consolidation cycle, due to a larger $u_{\text{thresh}}=10^{-2}$.

distribution of the Esipov-Shapiro model, and shifting the biological details of that model away from the functional form of the diffusivity and into the functional forms of three separate kinetic coefficients. The result was a model that not only was more amenable to numerical simulation in two dimensions, but one for which closely related models could be analyzed mathematically.

A number of questions remained unanswered, however. First of all, it remains to be explicitly shown that the Medvedev-Kaper-Kopell (MKK) model indeed produces rings in two dimensions. Their analysis, as with Esipov and Shapiro's, was entirely one dimensional. Second, it would be interesting to see whether the MKK model reproduces the lack of entrainment of rings sometimes observed in colliding *Proteus* colonies. Furthermore, a physical understanding is

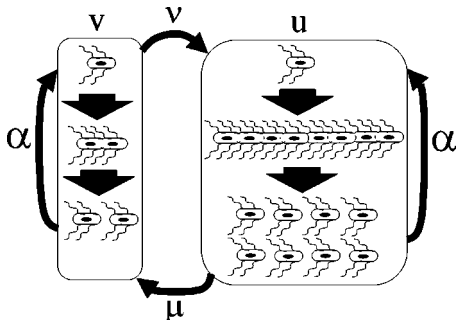

FIG. 2. Swarming life cycle. Cyclic differentiation-dedifferentiation life cycle of swarming bacteria. The rate constants shown in the figure illustrate the biological significance of the corresponding terms in the MKK equations (1). The bacteria are divided into two subpopulations: swimmers [with a biomass density $v(x,t)$ and swarmers (with a biomass density $u(x,t)$)]. The swimmers divide once they double in size; the swarmers delay division until they grow in length. Each of these subpopulations grows with an exponential growth rate $\alpha(v)$, modified by a differentiation of the short to the long papulation density (with a rate νv) and a dedifferentiation of the long to the short densities (with a rate μu). The functional form of these rates is illustrated in Fig. 3.

desired of the emergence of a spike in the spatial profile of the diffusivity that MKK found numerically and identified with the ring formation. It is not clear which of the biological details incorporated into the MKK model are required for the ring formation. Although MKK analyzed closely related equations in which the biological details were taken out, they stopped short of producing a final version of the model in which only the crucial experimental parameters were kept. Each of these issues prevent us from claiming that we understand the formation of bacterial colonial rings.

Review of Medvedev-Kaper-Kopell model

As described above, MKK reformulated the Esipov-Shapiro model by averaging over its swarmer age distribution. They maintain Esipov and Shapiro's partitioning of the bacteria into two subpopulations: a swimmer biomass density, $v(x,t)$, and a swarmer biomass density, $u(x,t)$. The resulting system of equations is as follows:

$$u_t(x,t)=\nu v(x,t)+(\alpha-\mu)u(x,t)+(D(u,v)u_x(x,t))_x,$$

$$v_t(x,t)=(\alpha-\nu)v(x,t)+\mu u(x,t), \tag{1}$$

$$D(u,v)=D_0\frac{u}{u+kv}.$$

The first of these equations gives the time rate of change of the swarmer biomass density as the sum of an exponential growth term (αu), the loss due to dedifferentiation of swarmers to swimmers $(-\mu u)$, and a diffusive flux to model the movement of swarmers. We will explore the nonlinear diffusivity they use below. The second of these equations gives the corresponding time rate of change of the nonmotile swimmer biomass density as the sum of an exponential growth term (αv) corresponding to swimmer

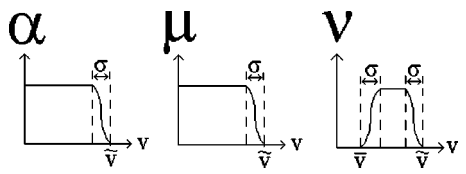

FIG. 3. Cartoon illustration of the functional dependence of the rate coefficients in the Medvedev-Kaper-Kopell model. Each varies with swimmer density $v(x,t)$. To aid mathematical analysis, the authors of Ref. [6] gave the transitions widths of σ. Each of these rates drop to zero above an upper swimmer density threshold $\tilde{v}$. In addition, the differentiation rate $\nu(v)$ receives a lower cutoff of $\bar{v}$, below which the differentiation rate goes to zero. In each case, the versions of the coefficients we used in our numerical integrations below had the transition regions implemented with straight line segments: unless otherwise noted, we used $\bar{v}=12.0$ and $\tilde{v}=16.0$, in accordance with the parameters used in Ref. [6], and we chose $\sigma=0.1$. If (a) The total biomass growth rate $\alpha(v)$. (b) The dedifferentiation rate $\mu(v)$, the rate at which swarmers dedifferentiate to swimmers. (c) The differentiation rate $\nu(v)$, the rate at which swimmers differentiate to swarmers.

cell division, a loss due to differentiation of swimmers to swarmers $(-\nu v)$, and a gain due to dedifferentiation of swarmers to swimmers (μu). With the third equation, MKK took for the diffusivity a weighted fraction of biomass in the swarmers, with the swimmers weighted with a factor of $k>1$ to account for the enhanced motility of the swarmers.

This functional form for the nonlinear diffusivity is biologically reasonable. If we interpret k to be the average ratio of long (swarmer) to short (swimmer) bacterial lengths, the given weighted fraction is the fraction of bacterial population members (i.e., entire cells) that are swarmers, rather than the fraction $u/(u+v)$ of biomass concentrated in swarmers. This functional form also has properties consistent with experiment. First, motility continues despite decreasing swarmer density during expansion. The form of the MKK diffusivity accounts for this, in that it remains finite as swarmer density (u) decreases. Second, the swarmer density does not drop to zero when swarming stops. This is again accounted for by the MKK diffusivity: this diffusivity can approach zero (stopping swarming) with a finite swarmer density as long as the ratio of swimmer to swarmer densities, v/u, diverges. Finally, the swarming motility decreases with increasing swimmer density. This is consistent with the fact that the MKK diffusivity approaches zero for large swimmer density v.

The biological details that Esipov and Shapiro incorporated into the nonlinear diffusivity, MKK incorporated into the functional forms of their rate coefficients. These are the total biomass growth rate $\alpha(v)$, the dedifferentiation rate $\mu(v)$ of swarmers back to swimmers, and the differentiation rate $\nu(v)$ of swimmers to swarmers. These are illustrated in Fig. 3. The upper cutoffs on each of these coefficients were intended to halt all bacterial growth above a maximal swimmer density $\tilde{v}$. This effect is in accordance with the experimental observation that bacterial growth saturates, no matter how much food is present. However, we have shown elsewhere [7] that only the upper cutoff on the overall growth rate, $\alpha(v)$, is required for this purpose; the upper cutoffs on the other two coefficients do not alter the behavior of the model.

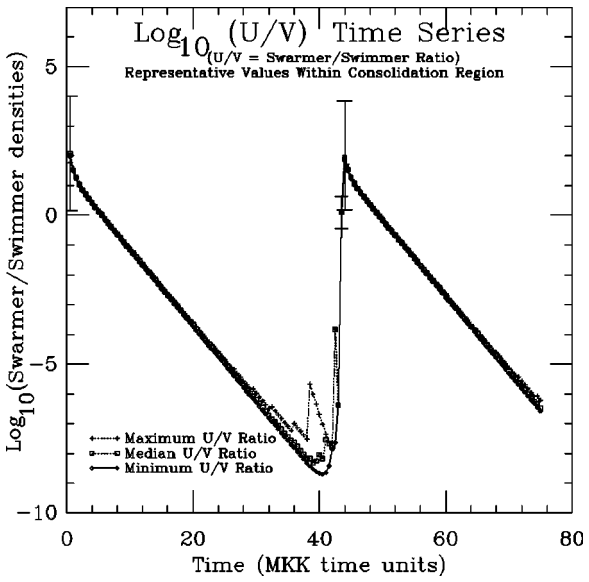

FIG. 4. Time series of representative values of the swarmer to swimmer ratio, u/v. Representative values of the swarmer to swimmer ratio u/v are plotted as a function of time, for the MKK model equation (1), as amended by Eq. (2), with the same parameters as reported above. Plotted are logarithmic (base 10) values of the maximum, median, and minimum values of the swarmer to swimmer ratio, u/v, within the consolidation region. For this purpose, the consolidation region is approximated as that region between an inner radius, where $u=u_{\mathrm{consol}}$, and an outer radius, where $u=u_{\mathrm{thresh}}$. It can be seen that the differences between the maximum, median, and minimum values of the ratio u/v at any given time are insignificant compared to the differences in these values introduced by time evolution. As a result, the time series of $\log_{10}(u/v)$ values takes the form of a well-defined sawtooth curve, with nearly vertical linear rises and relatively shallow linear declines. These linear rises and falls on this log plot correspond to exponential increases and decreases of the u/v ratio itself. The fast upward rise occurs during the same time interval as the swarming phase, and the relatively slow downward fall occurs during the same time interval as the consolidation phase. It should be noted that this plot shows that the ratio u/v is small $(\ll 1)$ during consolidation, in agreement with the mid-consolidation phase snapshot of the profiles shown in Figs. 7(b) and 7(c). We have analytically calculated [7] the slope of the downward segments of this plot and found it to be $-\mu/\ln 0$, which agrees with the plots presented here.

In addition, the differentiation rate $\nu(v)$, the rate at which swimmers differentiate to swarmers, has a lower cutoff of $\bar{v}$, below which the differentiation rate goes to zero. This corresponds to an experimentally observed initial latency in swarmer cell production when a colony first starts growing from an inoculum. Until the density of swimmers reaches a threshold, swarmers do not appear. In addition, the upper cutoffs, in combination with the lower cutoff on the differentiation rate, allow the swarmer density to approach zero through diffusion (without being replaced by newly formed biomass). This allows the diffusivity to approach zero and thus slow the expansion of the colony.

MKK numerically integrated their equations [Eqs. (1)],

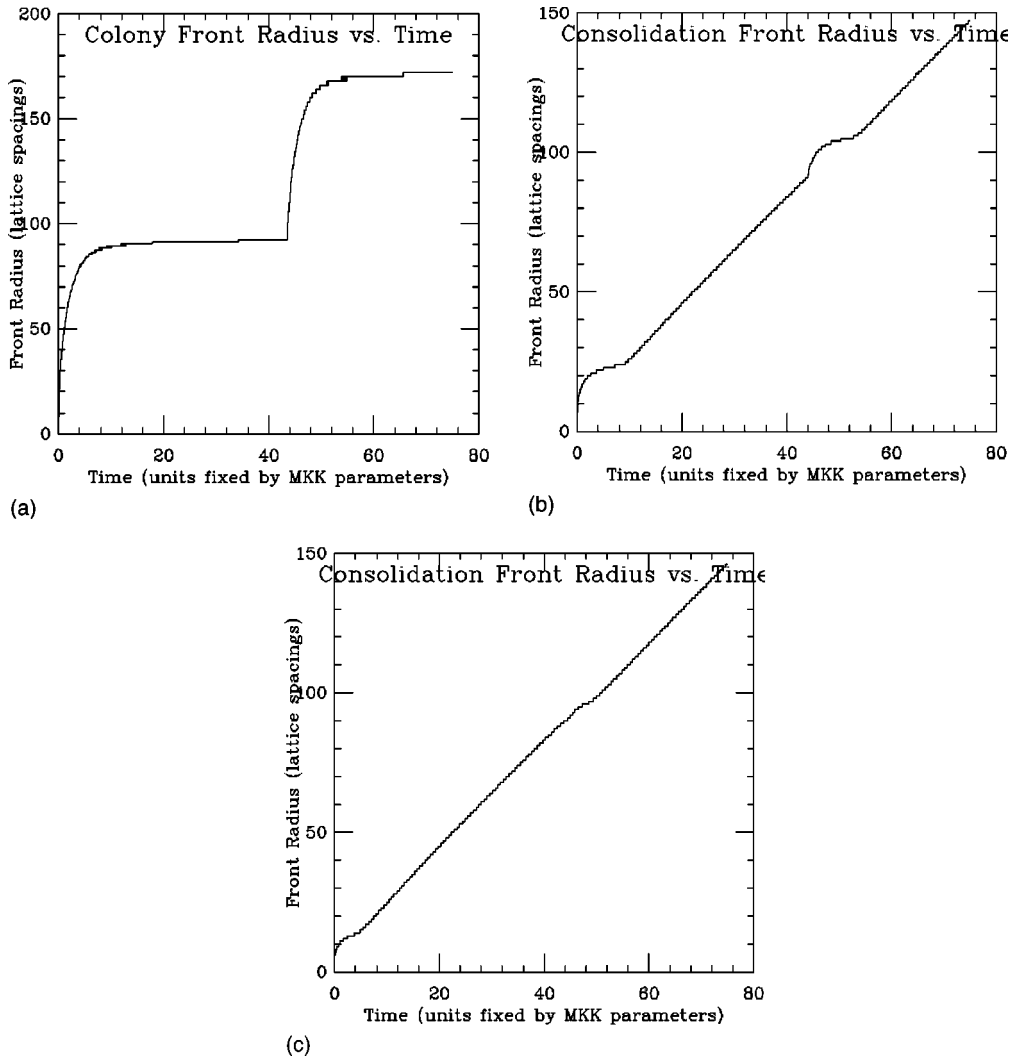

FIG. 5. Time series of the radii of the entire colony and of the consolidation front. These are results from numerical integration of the MKK equations (1), as amended by Eq. 2. Parameters used were $D_0=25$, $\alpha=0.7$, $\mu=\nu=0.6$, $k=5$, $\overline{v}=12$, $\tilde{v}=16$, and $u_{\text{thresh}}=10^{-10}$. Error bars are are not presented, as the radius is determined as the lattice site where the averaged radial profile dips below some threshold. The initial condition we use in this and other figures we borrow from the code of MKK. The swimmer and swarmer densities are constant within a radius of five lattice units of the colony center, and zero otherwise. The swimmer density is set to a value of 11.5 within this region, and the swarmer density to 9.0. Although this differs from biologically relevant initial conditions, in which the swarmers start at zero everywhere, numerical results (data not shown) indicate that the colony radius does not increase significantly until the swarmer density is built up. (a) The colony front is defined as the spatial location at which the swarmer (u) profile first dips below $u_{\text{thresh}}=10^{-10}$. Note that growth of the colony front occurs in bursts, in agreement with both experimental and previous numerical results. (b) The consolidation front is defined (somewhat arbitrarily) as the spatial location at which the swarmer (u) profile first dips below the threshold of $u_{\text{consol}}=10^{-1}$. This value was chosen because it was near the inner edge of the exponentially decaying part of the swarmer density distribution of Fig. 7(b). The focus of attention is not the series of bumps in this plot, but rather the linearity of the majority of the plot. These linear segments indicate that consolidation front propagation occurs at a constant velocity. The slope of the linear portions of this curve (that is, the observed consolidation front velocity) is approximately 1.93 ± 0.05 lattice units per MKK time unit. (c) The same consolidation front time series as in (b), but with a larger $u_{\text{consol}}=1.0$. The deviations from linearity that appeared in (b) are barely recognizable, indicating that the consolidation front appears to propagate linearly with time even during swarming.

and identified a significant physical insight to the mechanism of ring formation. The striking thing they found was the presence of a spike in the profile of the diffusivity that formed at the colony front just before the swarming phase began. According to Eq. (1), this implies a spike in swarmer cell density just before swarming starts. In support of this, Rauprich *et al.* [1] observed that the leading edges of swarming *Proteus* colonies were composed of populations four to five cells thick, whereas just behind the growing front, the population was only a single cell thick. MKK also produced a colony radius vs time plot demonstrating that their model yielded growth that was not just cyclic, but indeed occurred in bursts. With the MKK model in hand, we are ready to explore some of the issues we raised in Sec. I: rings in two dimensions, entrainment of colliding rings, identification of crucial biological details.

II. NUMERICAL STUDIES OF MKK MODEL

A. Correcting the MKK model

We first reproduced the numerical observations of MKK similar to our Fig. 1(b). We determined that they used a significant but undocumented modification to the analytic model they presented: they implemented a lower threshold on the swarmer density, below which they set it to zero. We determined that this threshold was crucial to the ring generation mechanism.

This swarmer density diffusivity threshold is biologically reasonable: it accounts for the physical discreteness of the distinct bacteria. If the swarmer density goes below some level corresponding to a single bacterial layer, for example, the corresponding decrease in bacteria-bacteria interactions would reduce the enhanced motility due to bacterial entanglement. It is thus a valid biological feature that the swarmer density diffusivity should approach zero for as the swarmer density approaches some finite but small threshold value from above.

We use an alternating-direction-implicit method in conjunction with a forward-time, centered spacing technique of finite differencing in our numerical integration of the MKK equations. In Fig. 4 we present our numerical results for the time evolution of the swarmer to swimmer ratio u/v in the region near the front (where u and v approach zero). We see there that the ratio u/v in the consolidation region decays exponentially (with a decay rate μ [7]) for the entire duration of the consolidation phase. This observation provides a quantitative constant to the behavior of the swarm-consolidation cycle (see Fig. 1).

The large u/v ratio observed in Fig. 4 during swarming can be understood as follows. Recall that the swarmers (u) are motile, while the swimmers (v) are immotile and must wait for the swarmers to populate an area before the swimmer density can build up. During the swarming phase, i.e., before the swimmer (v) density has caught up to the swarmer (u) density in newly populated areas, the ratio u/v is therefore large. Equation (9) then indicates that, very near the front (i.e., as both u and v approach zero), $D(u,v) \rightarrow D_0(u/\epsilon) \rightarrow 0$ rather than the correct form of $D(u,v) \rightarrow D_0(u/u) = D_0$. The specific form in which MKK handled this limit of the expression for the diffusivity thus has the heretofore undocumented effect of artificially decreasing the diffusivity to zero (rather than to D_0) near the front.

We found that this detail was crucial to the abrupt bursts of growth shown in Fig. 1(b). We therefore explicitly build it into the model with the following expression for the diffusivity, in which diffusivity is explicitly set to zero when the swarmer (u) density falls below some threshold u_{thresh}:

$$D(u,v) = D_0 \frac{u}{u+kv} \Theta(u - u_{\text{thresh}}). \tag{2}$$

We will see below that the value of this threshold, u_{thresh}, directly controls the period of the swarm plus consolidation cycle. We proceed using the corrected MKK model, consisting of Eqs. (1) as modified by Eq. (2).

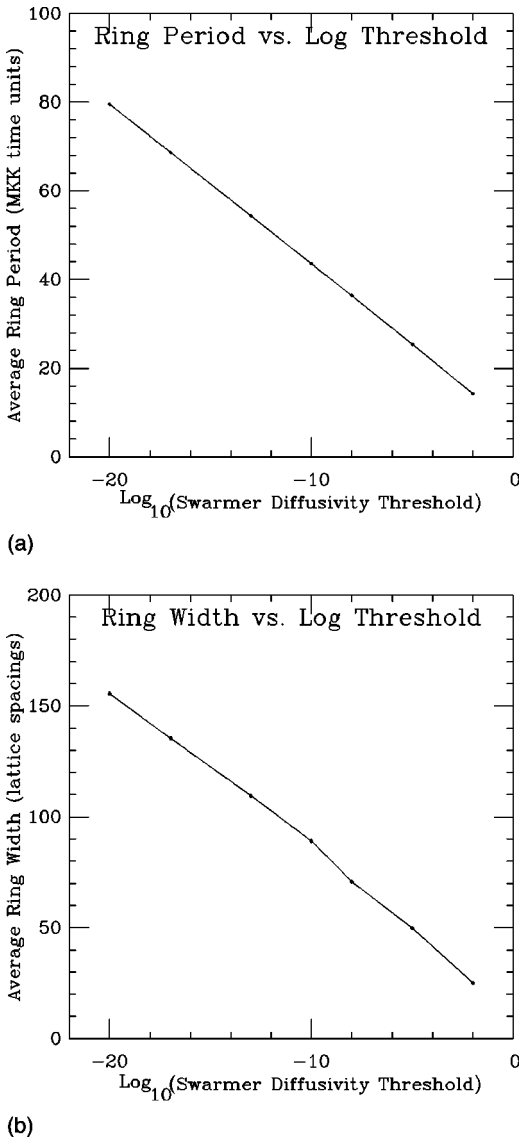

FIG. 6. Illustration of exponential decay of ring period and width with the swarmer density diffusivity threshold. The swarmer density diffusivity threshold u_{thresh} of the diffusivity expression in Eq. (2) is varied, and the corresponding (average) ring period and width is observed. Shown are (a) the ring period, and (b) the ring width, both as functions of $\log_{10}(u_{\text{thresh}})$. For both of these plots, it can be seen that, consistent with the rings illustrated in the colony radius time series plots of Fig. 1, the ring period and width both decrease exponentially with the swarmer density diffusivity threshold.

B. Effect of the swarmer density diffusivity threshold

We illustrate in Figs. 1 and 6 the effect of varying the swarmer density threshold u_{thresh} of the diffusivity expression in Eq. (2). In Fig. 5 we see the qualitative effect on the colony radius time series of increasing the swarmer density diffusivity threshold u_{thresh} several orders of magnitude. We examine the effects of u_{thresh} in terms of ring period and width. A *ring* here refers to that part of colony growth that occurs during a swarm plus consolidation cycle. *Ring period* refers to the amount of time between the abrupt initiations of

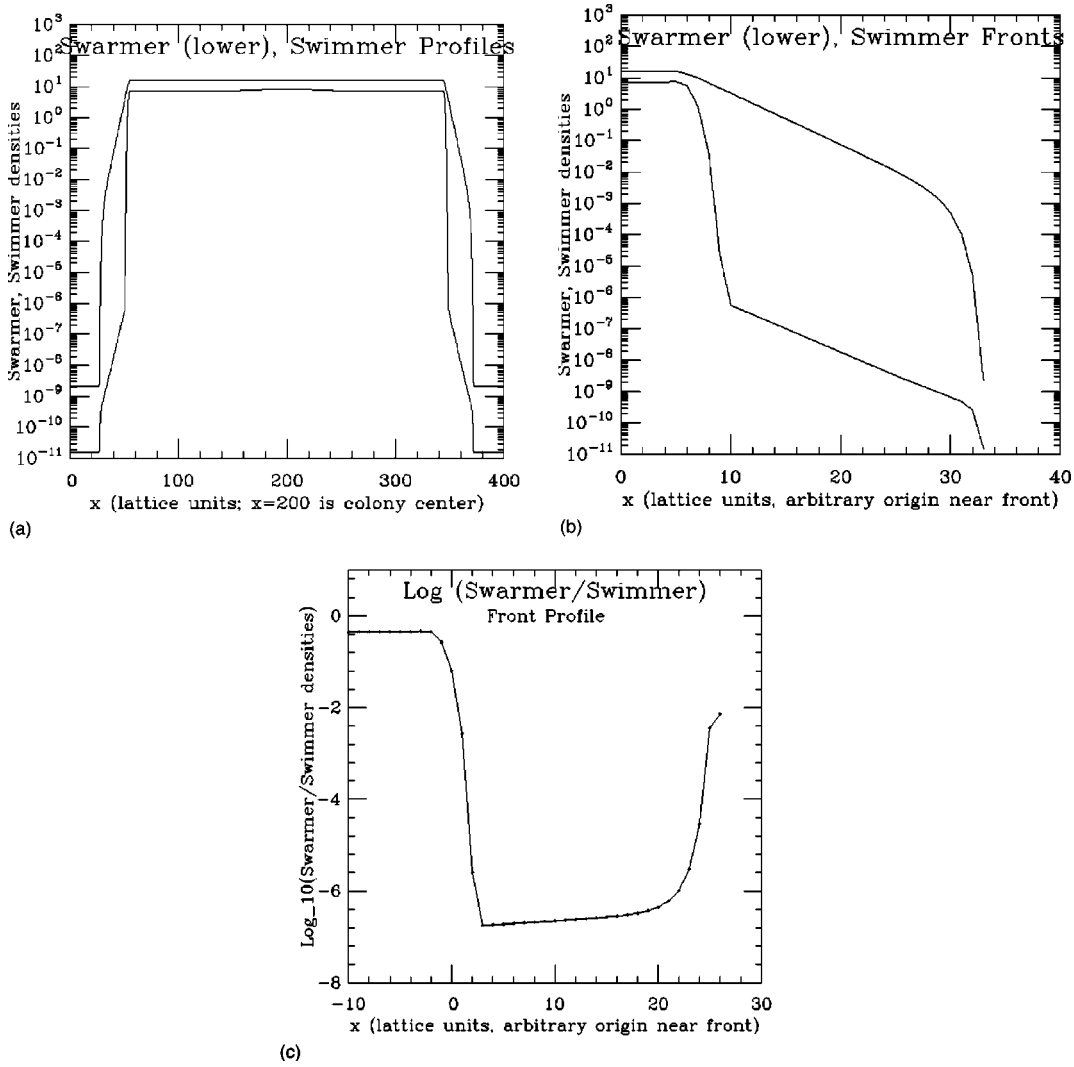

FIG. 7. Illustration of the exponential decay of bacterial densities in the consolidation region in the MKK model. Shown are the exponential decay of bacterial densities resulting from the MKK model [Eq. (1)] as amended by the second equation below [for ((a) and (b))] and Eq. (2) [for (c)]. Shown are logarithmic (base 10) plots of swarmer (u) and swimmer (v) density profiles and [in (c)] their ratio in midconsolidation phase. In (c), the region (near the origin) over which the u/v ratio undergoes a steep decay propagates outward during consolidation until it reaches the corresponding peak at the colony radius: this leads to formation of the diffusivity spike observed in Ref. [6], and the induction of swarming. In each figure, error bars are based on scatter in the plotted quantities and are below the resolution of the plot. MKK implemented the nonlinear diffusivity in their model through the combinations

$$D(u,v)=D_0\frac{u}{u+kv+\epsilon},\ u=u\Theta(u-u_{\mathrm{thresh}}),$$

with ϵ a small constant, $\epsilon=10^{-11}$. For (a) and (b), we implement a slight variant of these modifications

$$D(u,v)=D_0\frac{u}{u+kv+\epsilon}\Theta(u-u_{\mathrm{thresh}}).$$

Parameters used were $D_0=25$, $\alpha=0.7$, $\mu=\nu=0.6$, $k=5$, $\bar{v}=12$, $\tilde{v}=16$, and $u_{\mathrm{thresh}}=10^{-10}$. (a) The full profiles: the top curve is the swimmer (v) density; the lower curve is the swarmer (u) density. We maintain the full profile in our code, rather than just the $x\geqslant 0$ region, in anticipation of integrating the corrected MKK equations in two dimensions. (b) The profiles near the front, in what we call the consolidation region. Note that the spatial decay rates of both swimmers and swarmers are the same within much of the consolidation region. (c) The ratio of the profiles near the front. The steep increase in (the logarithm of) this value at the colony front remains at the front during consolidation, and underlies the small precursors to the diffusivity spike observed by MKK. This precursor remains stationary at the front while the consolidation front propagates outward. When the consolidation front catches up to the colony front, the previously observed diffusivity spike appears, and initiates a new swarming phase. Note that in this midconsolidation phase snapshot of the ratio profile, the value of the ratio is $\ll 1$ throughout the consolidation region.

growth defining the start of the swarming phases at the beginning of the current and the succeeding ring. Similarly, *ring width* refers to the distance between the colony radius at these two times. With this terminology, Fig. 1 demonstrates the qualitative observation that ring period and ring width both decrease with an increase in u_{thresh}.

In Fig. 6, we quantify this decrease of ring period and width with increases in u_{thresh}. There we plot ring period and ring width as a function of $\log_{10}(u_{\text{thresh}})$. We see that ring period and width both decrease exponentially with the swarmer density diffusivity threshold. This can be interpreted in terms of observations we have made above.

C. Effect of kinetic coefficient cutoffs

The upper thresholds $\tilde{v}$ on the differentiation rate $\nu(v)$, the dedifferentiation rate $\mu(v)$, and the growth rate $\alpha(v)$, collectively serve to prevent the bacterial densities from increasing without bound. As a simplification, we verified that we could achieve the same effect with the upper threshold only on the growth rate, $\alpha(v)$. For consistency, however, we do not use this simplification throughout.

D. Observation of rings in the colony interior

If the MKK model is to be used to model experimentally observed bacterial rings, it must yield not only the bursts of growth illustrated in Fig. 1(b), but also latent effects of those bursts of growth in the form of rings in the bacterial density profiles within the colony, away from the front. Plots illustrating the amplitude of the rings in the radial bacterial density distribution relative to the background bacterial density do not appear to be available in the literature. This is probably because experimenters view the rings by scattering light off the colony. This technique certainly locates the position of the rings, but it does not yield an estimate of their relative bacterial density from the height of the rings above the colony surface. However, microscopic observations (by Rauprich *et al.*, for example [1]) indicate that, at least near the colony edge, the bacterial densities are so small that the approximation of bacterial dynamics near the edge with continuous differential equations is questionable. For example, they observe 4–5 bacterial layers at the propagating front, and only a single layer just inside the front. We have not found published data indicating the corresponding number of bacterial layers at the location of the rings far from the colony edge.

Despite this lack of quantitative biological experimental data, we can still look for the presence in the MKK model of any rings at all left in the bacterial distribution far from the colony front. Figure 7(a) shows that if there are any such rings left in the profile, they are not large compared to the background density. This leads us to search harder for any evidence of rings in the profiles.

In Fig. 9, we make a color plot of the two-dimensional swarmer bacterial density distribution resulting from the corrected MKK equations in two dimensions. The rings evident there in the colony interior allow us to use the MKK model to probe two-dimensional experimental observations of the rings, such those of colliding colonies and of branched rings.

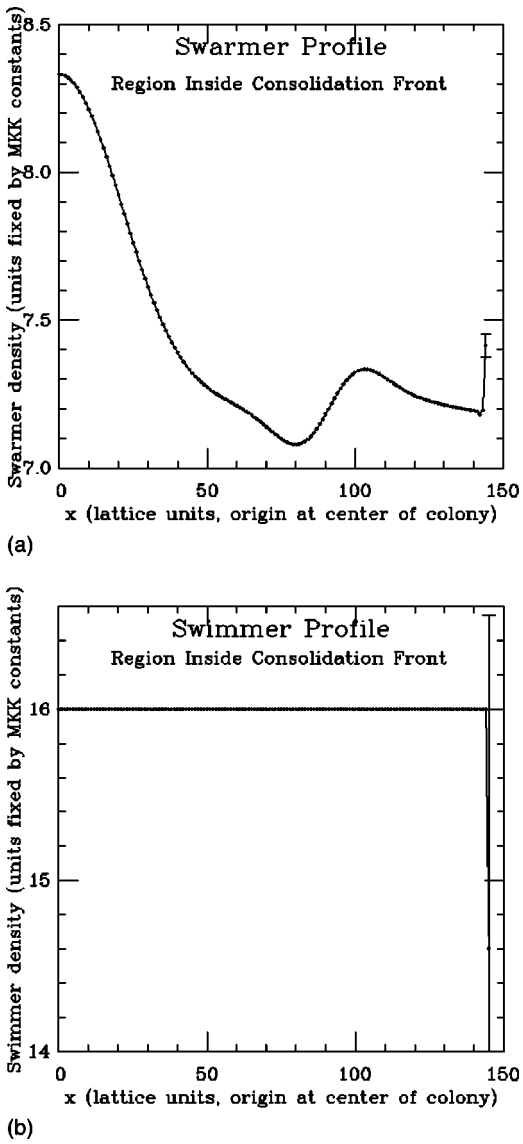

FIG. 8. Macroscopic remnants in the bacterial density profiles of the bursts of growth associated with swarming. Density profiles are plotted on a linear scale for the interior of the colony, which includes the entire colony except for the consolidation region: these plots thus include the entire domain of the colony. Parameters used were as in previous figures. The features in these plots illustrate the relatively small details in the structure of these profiles. The profiles are plotted at the same midconsolidation phase time at which previous profile plots were made. (a) The swarmer density profile within the colony interior. Note the presence of a small peak [with relative magnitude $\delta u/u = O(10^{-2})$] in the region $x = 80-120$ lattice spacings corresponding to the burst of growth that at roughly $t = 45$ MKK time units that appears in Fig. 5(a). (b) The swimmer density profile within the colony interior. Note that this profile is constant in the interior; this constant is the upper threshold, $\tilde{v}$, on on the MKK coefficients (illustrated in Fig. 3).

III. EXTENSION OF MKK TO TWO DIMENSIONS

Recall that one of our original goals was to model the two-dimensional (2D) ring patterns observed in the real bacterial systems. To this end, we now run two-dimensional

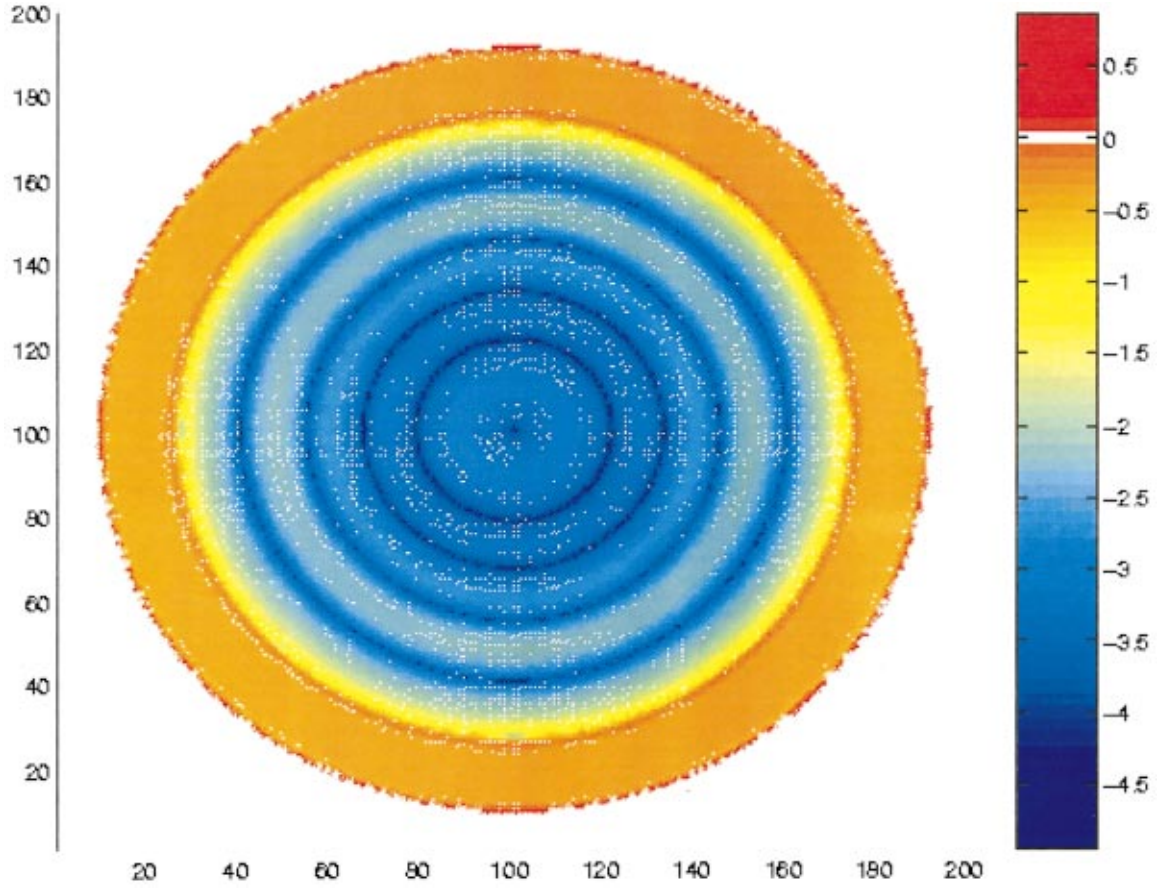

FIG. 9. (Color) Color map illustrating the magnitude of the swarmer bacterial density gradient. A color plot of the logarithm (base 10) of the magnitude of the bacterial density gradient, normalized to the local density η of Eq. 3. The results presented here correspond to a simulation run with swarmer diffusivity threshold $u_{\text{thresh}}=10^{-2}$. Note that the colony perimeter is smooth, not branched. Note also that the rings in this figure correspond to local extrema of the respective bacterial densities: they are where the peaks and troughs are in the bacterial distribution, rather than where the edges of the rings are.

versions of our simulation to determine whether rings are still formed and to determine whether the MKK model produces branching patterns in two dimensions.

We plot the magnitude of the gradient of the bacterial densities to view the ring remnants on the colony interior. Because the rings only leave relatively small artifacts in the bacterial densities on the interior of the colony (as in Sec. II D), we cannot view these features directly with a contour map of the bacterial density. We therefore calculate the above mentioned gradient magnitude, normalize it to the local bacterial density, and plot its logarithm (base 10). We illustrate typical results of this technique in Figs. 11(a) and 11(b).

A. Visualizing the 2D structure of the rings

We first verify (results not shown) that the MKK model produces the same type of ring formation we found in the one dimensional version of the simulation. The colony front radius continues to propagate outward in bursts, a consolidation front still exists and propagates outward linearly except at the onset of swarming, and the swarmer to swimmer density ratio in the consolidation front decreases exponentially except during the onset of swarming.

Now that we know the MKK model produces rings in two dimensions, the next question is, what do these rings look like? Although the (root mean squared) colony radius (as defined with a swarmer threshold u_{thresh}) expand outward in bursts of swarming and consolidation, what is the shape of the propagating front? Is it smooth, corresponding to the patterns observed in *Proteus*, or branched, corresponding to those observed in *Bacillus*?

To answer these questions, we need a method of viewing the full, two dimensional bacterial density distributions in the simulated colonies. Figure 8 illustrates that, at least for the simulation parameters we are using, the relative amplitude of the rings left in the colony interior is only of the order of 1% of the peak amplitude. (We will discuss this quantity later, in Sec. III D.) A simple contour plot would therefore fail to illustrate the ring remnants on the colony interior.

We therefore implement a different method of visualizing the ring remnants. We calculate the radial gradient of the bacterial densities: the spatial gradient in the direction radially outward from the colony center. We then normalize to the local field value. Finally, we plot the resulting quantity

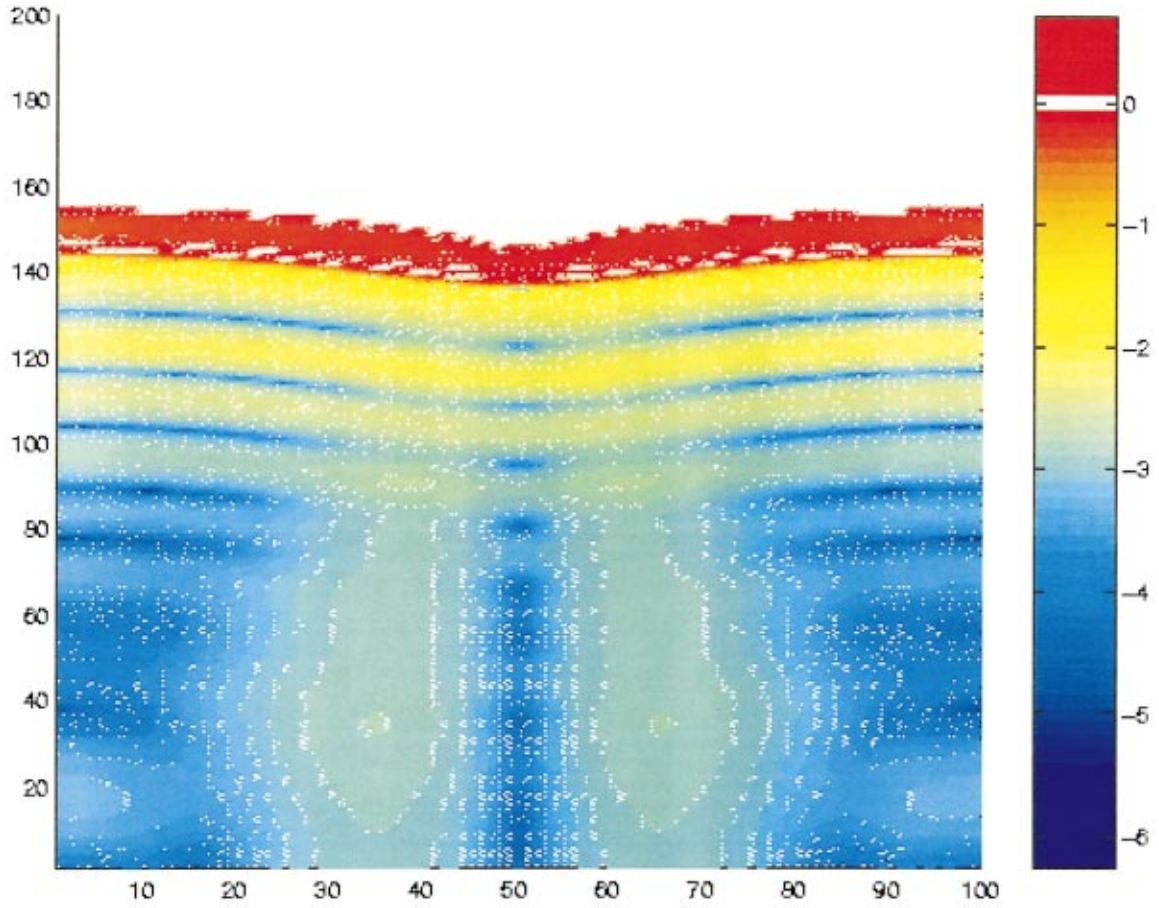

FIG. 10. (Color) Color map illustrating the magnitude of the gradient of the swarmer bacterial density for two ring colonies grown in phase. A color plot of the logarithm (base 10) of the magnitude of the gradient of the swarmer bacterial density, as in Fig. 9. The two colonies are grown in phase: both the bottom-left and bottom-right colonies start growing at $t=0$. The initial conditions of each of these colonies are identical: they each start in the midswarming phase. The gradient magnitude of the swarmer density is shown at $t=85.0$. This plot demonstrates that the two colonies have merged both at the periphery and deep in the colony interior.

$$\eta \equiv \log_{10}\left(\frac{\sqrt{[(\partial u/\partial x)(x,y,t)]^2+[(\partial u/\partial y)(x,y,t)]^2}}{u(x,y)} \right), \tag{3}$$

with a color scale. We note from the two-dimensional simulation with results in Fig. 9 that the rings are smooth rather than branched.

B. Experiments with colliding colonies

The next question we address is, do the rings from two separate colonies merge or remain distinct? Biological observations indicate that the rings merge if the colonies are in phase [i.e., both in the same growth phase (swarming or consolidation)], and that they remain distinct if the colonies are out of phase.

Here we simulate two colonies with their growth phases either in phase or out of phase. We grow one colony in the bottom-left corner of the simulation region, and one in the bottom-right corner. These colonial positions allow us to produce pictures of colliding colonies computationally efficiently.

For an in-phase diagram, we initiate growth in the two colonies at the same time and with the same initial conditions. For an out-of-phase diagram, we initiate the growth in the bottom-left colony in the midswarming phase, and we initiate that in the bottom-right colony in the same midswarming state only after the first colony has entered midconsolidation phase. (We typically initiated the second colony at $t=7.5$ MKK time units.) We illustrate the result of the in-phase experiment in Fig. 10, and that for the out-of-phase experiment in Fig. 11.

We see in the case for which the colonies are grown in phase (Fig. 11), that the two colonies have clearly merged both at the periphery and far behind the propagating front. This is consistent with the experimental observation that in-phase colonies merge, a process called entrainment.

On the other hand, we see, in the out-of-phase case, (Fig. 10), that the two colonies have clearly not merged at the periphery, and we see less clearly that they do not appear to have merged far behind the propagating front. This is consistent with the experimental observation that out-of-phase colonies do not merge.

It thus appears that the MKK model predicts that ring colonies grown in phase merge and those grown out of phase

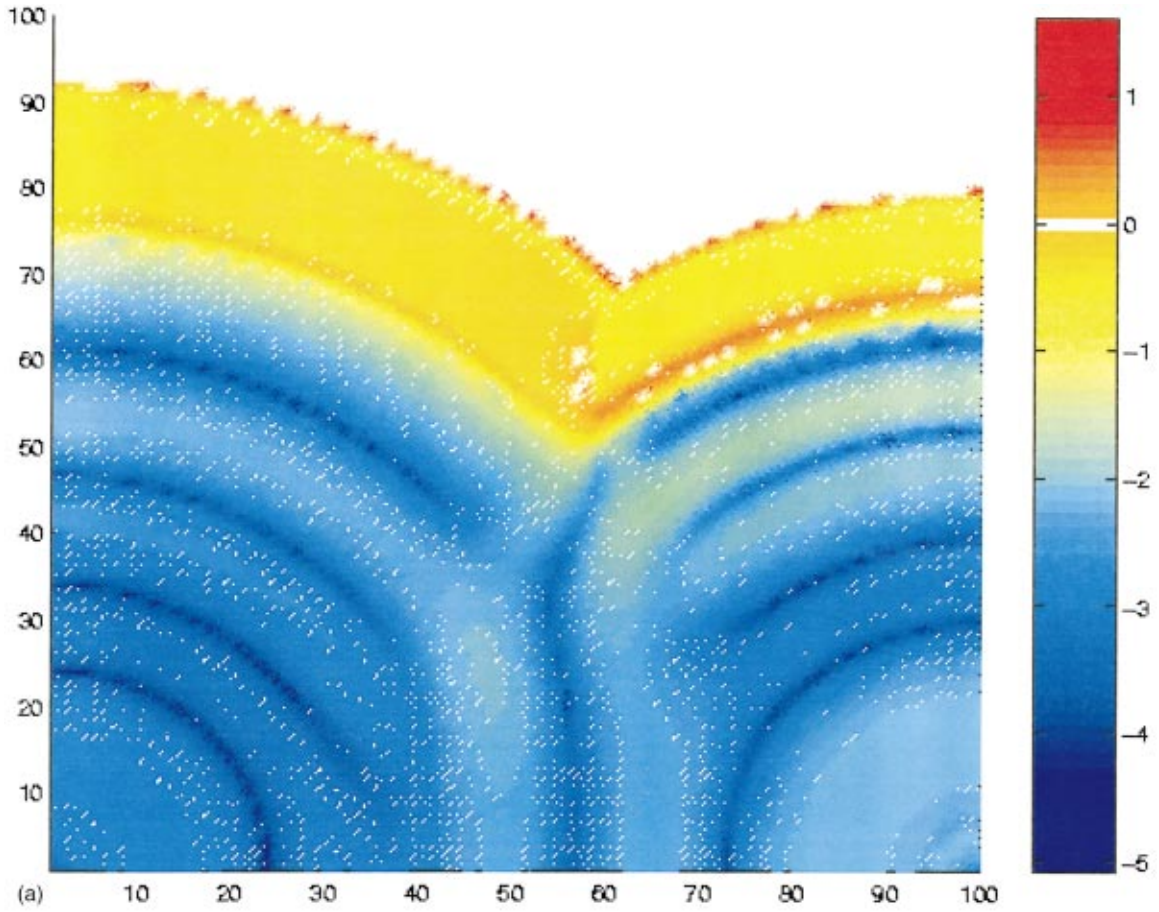

FIG. 11. (Color) Color map illustrating the magnitude of the gradient of the bacterial densities for two ring colonies grown out of phase. A color plot of the logarithm (base 10) of the magnitude of the gradient of the bacterial densities, as in Fig. 9. The two colonies are grown out of phase: in each figure, the bottom-left colony starts growing at $t=0$, and the bottom-right one at $t=7.5$. The initial conditions of each of these colonies are identical: they each start in the midswarming phase. The time delay between the two is such that the initial swarming phase of the later colony occurs in the middle of the first consolidation phase of the earlier colony. (a) The gradient magnitude of the swarmer density, $u(x,y,t)$, at $t=43.5$. At this time, the earlier (lower-left) colony is in the midswarming phase. This plot may indicate that the two colonies have not even merged far behind the propagating front. (b) The gradient magnitude of the swimmer density, $v(x,y,t)$, at the same time as in (a). The discontinuity in the contours of the two colonies indicate that the two colonies have not merged at the periphery.

remain distinct but may merge deep in the colony interior. It would be nice to quantify the distinction between in and out of phase. However, we lack a quantitative measure for whether a given ring has merged. We therefore can only produce pictures of predictions, rather than analytic predictions for experiment.

C. Model for branched rings

Rings have been observed in real biological systems to coexist with branching colony envelopes, as in the branched rings of *Bacillus* [4]. Here we introduce a model yielding branching patterns in conjunction with rings generated by the MKK mechanism. We induce branching in the MKK model by coupling the bacterial fields to a limited nutrient field, a technique used extensively in modeling branching bacterial colonies [8–18]. We find that the correspondingly modified MKK equations contain a Mullins-Sekerka instability.

The nutrient evolution equation we use is as follows: We introduce a nutrient field density $n(x,y,t)$ with an evolution equation incorporating the eating of food by the all bacteria (swimmers or swarmers) and the diffusion of nutrients:

$$n_t = -\lambda \alpha_{\max} n(u+v) + D_n n_{xx}. \tag{4}$$

Here λ is a conversion factor from biomass density to nutrient density, $\alpha_{\max}$ is the maximal value of the MKK coefficient $\alpha(v)$, and D_n is a constant nutrient diffusivity. We typically use $\lambda=1$ or 3, $\alpha_{\max}=0.7$ (as in previous simulations), and $D_n=D_0$ (nutrient diffusivity coefficient equal to the maximal swarmer diffusivity).

We motivate this nutrient evolution equation based on the standard MKK model by calculating the rate of change of the total biomass (swarmer plus swimmer biomass density). We add the bacterial density equations from Eqs. (1):

$$w(x,t) \equiv u(x,t) + v(x,t),$$

$$w_t(x,t) = \alpha(v(x,t))w(x,t) + (D(u,v)u_x(x,t))_x. \tag{5}$$

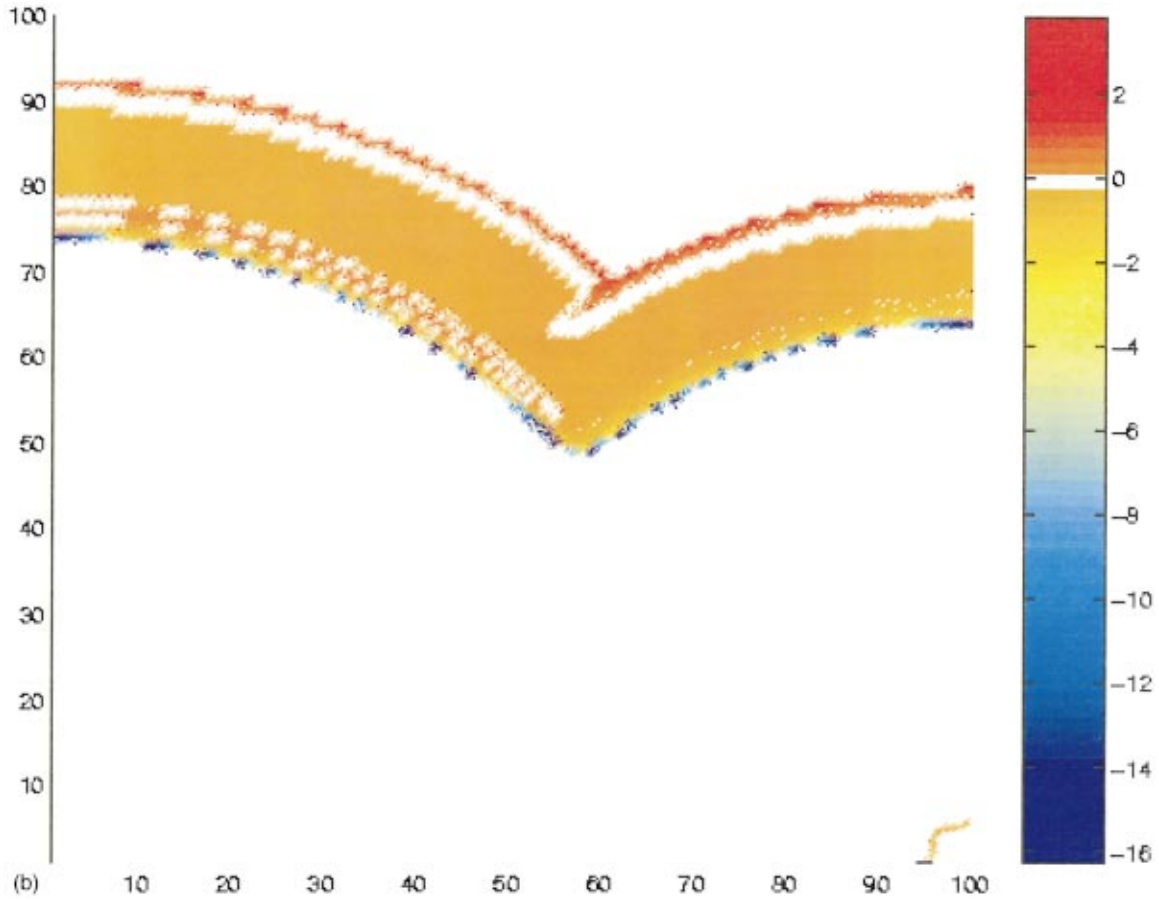

FIG. 11. (*Continued*).

That portion of this total biomass density change not due to bacterial flux must be modulated by the nutrient field. Therefore, we may incorporate the effect of the nutrient field into the MKK growth coefficient $\alpha(v)$: $\alpha(v)\rightarrow\alpha(v,n)$. To date, the only nontrivial feature of this coefficient, an upper swimmer density threshold, had the effect of limiting bacterial growth. Now we want nutrient limitation to limit this growth. We can therefore create a function $\alpha(n)$ to mimic this effect.

Therefore, we replace the upper cutoff $\tilde{v}$ in the original $\alpha(v)$ (pictured in Fig. 3) with a nutrient density modulation,

$$\alpha(v)\rightarrow\alpha(n)=\alpha_0 n C_{\text{nutrient per biomass}}, \tag{6}$$

where $C_{\text{nutrient per biomass}}$ is a constant conversion factor between the bacterial density fields u and v and the nutrient density field n.

To complete the specification of the modification to the model, we provide initial and boundary conditions for the nutrient field $n(x,y,t)$. We choose as an initial condition a homogeneous nutrient density n_0 (which we typically take to be unity). We also impose hard wall (zero flux) boundary conditions at the edge of the plate. We implement the numerical integration of the additional (nutrient) field with a simple forward-time, centered spacing finite differencing scheme [19].

The resulting branched ring model is

$$\begin{aligned} u_t(x,t)&=\nu v(x,t)+(\alpha-\mu)u(x,t)+(D(u,v)u_x(x,t))_x,\\ v_t(x,t)&=(\alpha-\nu)v(x,t)+\mu u(x,t),\\ n_t(x,t)&=-\lambda\alpha_{\max}n(u+v)+D_n n_{xx},\\ D(u,v)&=D_0\frac{u}{u+kv}\Theta(u-u_{\text{threshhold}}), \end{aligned} \tag{7}$$

with α given by Eq. (6), and where we typically take $\lambda=C_{\text{nutrient per biomass}}$ from that equation. Numerical integration of these equations yield the desired branched ring patterns, as we illustrate in Fig. 12.

D. Significance of ring amplitudes

We noted in Sec. III A that the relative amplitude of the rings in our MKK simulations were only of the order of 1%, as shown in Fig. 8. It is unclear whether this order of magnitude disagrees with experiment. Indeed, Rauprich *et al.* [1] reported that, at least near the colony front, visually distinct bands of bacteria density differed only by a single bacterial layer. If the bacterial densities in the colony interior are of the order of 100 or more layers thick, which is not unreasonable, then the relative density fluctuations in our simulations are practical.

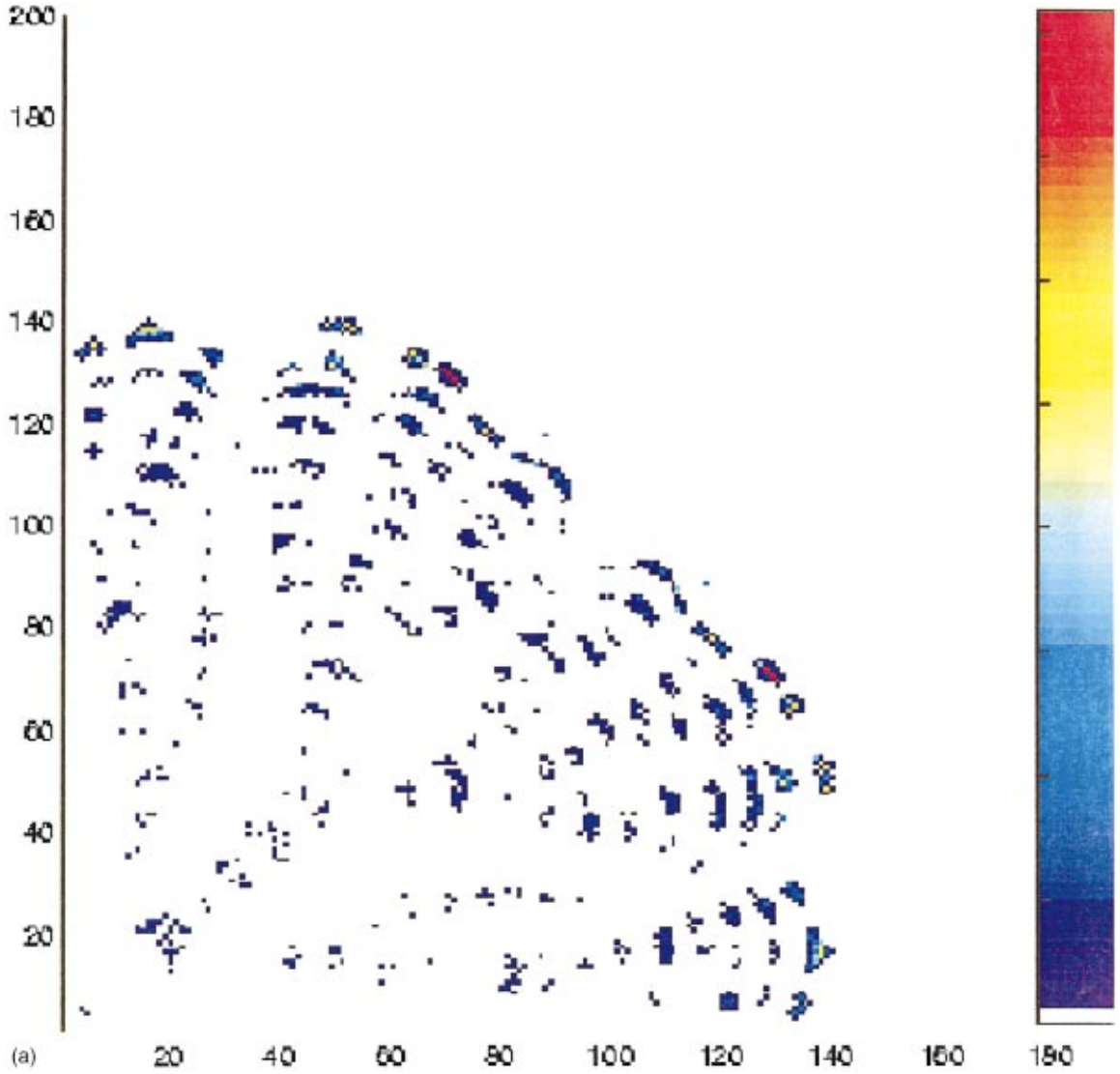

FIG. 12. (Color) Color maps illustrating branching ring patterns obtained from Eq. (7). Color plots of (a) the swarmer bacterial field density $u(x,y,t)$, and (b) the corresponding logarithm (base 10) of the normalized magnitude of the gradient of the swarmer density at the late time $t=600$ MKK time units. Note that the colony envelope illustrates both rings associated with the MKK mechanism and branches associated with nutrient limitation. The color of the entire colony appears uniform in (a) because the relative amplitude of the bacterial density at the colony front contains a peak.

If experiment shows that the relative density fluctuations are significantly larger than 1%, however, then we must identify a distinct method of obtaining such amplitudes. We identify two possible approaches: variation of our model parameters and weak nutrient limitation. We consider each of these approaches in turn.

We suspect that varying our model parameters could produce relatively larger bacterial density fluctuations at the location of the rings. This is so because we can vary our parameters to obtain a short cycle period (by increasing u_{thresh} and, we suspect, μ). The correspondingly smaller cycle period would give the bacterial kinetics less time to reach their equilibrium (consisting of constant values for u and v), especially in the consolidation region. We consider this the more appropriate option, although we did not study the regions of parameter space encompassing the correspondingly relatively short periods.

The other method for increasing the density fluctuation amplitudes associated with the rings is to add a weakened form of nutrient limitation. We found in Sec. III C that nutrient limitation yielded bacterial densities approaching zero between the rings. As we turn this effect off [e.g., $\lambda \to 0$, with $\alpha(n)$ a more steeply varying function of n to avoid bacterial density divergences], we expect rings of relatively larger density fluctuations. This method may disagree with experiment, however. If relatively large amplitude density fluctuations $[O(1\%)]$ are indeed observed in nutrient-rich environments, this method would not apply.

IV. SUMMARY

We have corrected the Medvedev-Kaper-Kopell model for bacterial ring formation to include a swarmer density diffusivity threshold. Although this feature did not appear in

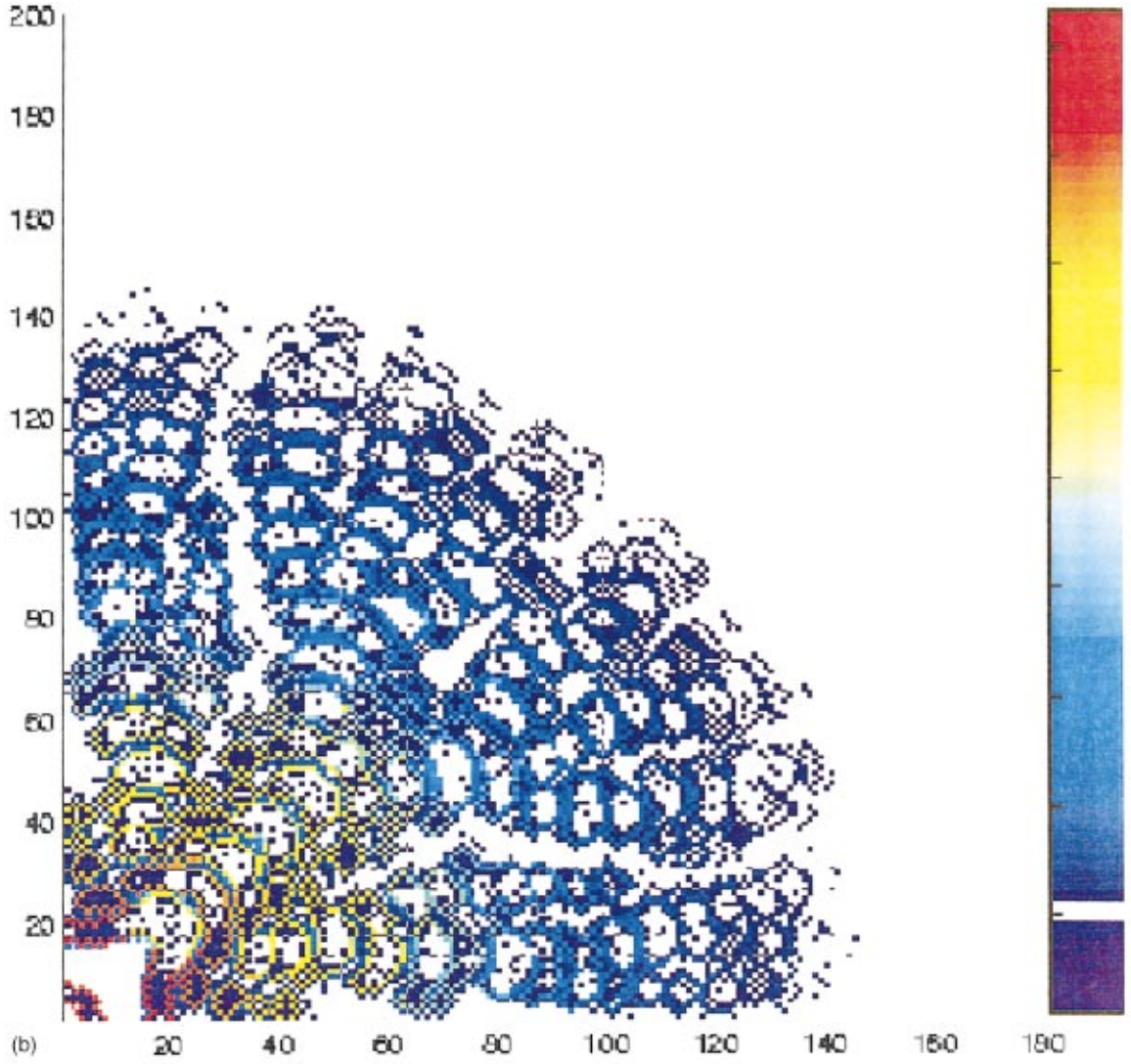

FIG. 12. (*Continued*).

(the uncorrected version of) the analytic form of the MKK model, it was crucial to the formation of rings in their results. This threshold was initially introduced as a cutoff for numerical stability, so its significance was unappreciated.

We further determined that this threshold determined the swarm plus consolidation cycle. This is a possible explanation of the experimentally observed independence of this cycle period on environmental growth conditions. We found that the logarithm of this swarmer density diffusivity threshold was directly proportional to the swarm plus consolidation cycle.

We also identified a pair of quantities that remain constant during the entire swarm plus consolidation cycle. These are the velocity of a ''consolidation front'' (which we defined, and whose significance we first appreciated) and the exponential decay rate of the swarmer to swimmer biomass density ratio within a ''consolidation region'' (which we also defined, and whose significance we first appreciated). These are the first constant behaviors of the system that have been identified during the entire swarm plus consolidation cycle.

We have also implemented the MKK model (as corrected with a swarmer density diffusivity threshold) in two dimensions. We demonstrated there that the resulting MKK model continues to yield rings, and we demonstrated that those rings contain a smooth, rather than a branched, interface. We also demonstrated the feasibility of the corrected MKK model to simulate experimental observations of colliding colonies experiments, namely, the entrainment of colonies growth in phase, and the lack of such entrainment for colonies grown out of phase. Finally, we extended the MKK model to simulate the branched rings observed in *Bacillus subtilis* by coupling the swarmer and swimmer bacterial densities to a nutrient field.

ACKNOWLEDGMENTS

Georgiy Medvedev graciously provided a copy of some of his code integrating the MKK equations. Without this help, we would probably have failed to reproduce any of the MKK results. We are also indebted to S. Esipov and J. Shapiro and to G. Medvedev, T. Kaper, and N. Kopell for making available preprints of their papers.

[1] O. Rauprich, M. Matsushita, C. Weijer, F. Siegert, S. Esipov, and J. Shapiro, J. Bacteriol. **178**, 6525 (1996).
[2] Robert Belas, ASM News **58**, 15 (1992).
[3] L. McCarter and M. Silverman, Mol. Microbiol. **4**, 1057 (1990).
[4] I. Ràfols, M. Sc. thesis, Chuo University, Japan, 1998.
[5] S. Esipov and J. Shapiro (unpublished).
[6] G. Medvedev, T. Kaper, and N. Kopell (unpublished).
[7] Scott Arouh, Ph.D. thesis, University of California, San Diego, 2000.
[8] E. Ben-Jacob, H. Shmueli, O. Shochet, and A. Tenenbaum, Physica A **187**, 378 (1992).
[9] E. Ben-Jacob, Contemp. Phys. **38**, 205 (1997).
[10] I. Golding, Y. Kozlovsky, I. Cohen, and E. Ben-Jacob, Physica A **260**, 510 (1998).
[11] K. Kawasaki, A. Mochizuki, T. Matsushita, T. Umeda, and N. Shigesada, J. Theor. Biol. **188**, 177 (1997).
[12] S. Kitsunezaki, J. Phys. Soc. Jpn. **66**, 1554 (1997).
[13] D. Kessler and H. Levine, Nature (London) **394**, 556 (1998).
[14] H. Fujikawa and M. Matsushita, J. Phys. Soc. Jpn. **60**, 88 (1991).
[15] M. Matsushita, J. Wakita, H. Itoh, I. Ràfols, T. Matsuyama, H. Sakaguchi, and M. Mimura, Physica A **249**, 1 (1998); **249**, 517 (1998).
[16] M. Mimura, H. Sakaguchi, and M. Matsushita (unpublished).
[17] M. Mimura, H. Sakaguchi, and M. Matsushita (unpublished).
[18] M. Matsushita, J. Wakita, H. Itoh, I. Rafols, T. Matsuyama, H. Sakaguchi, and M. Mimura, Physica A **249**, 517 (1998).
[19] W. Press, S. Teukolsky, W. Vetterling, and B. Flannery, *Numerical Recipes in C: The Art of Scientific Computing*, 2nd ed. (Cambridge University Press, Cambridge, 1994), Chap. 19.